LRP 830/07 May 2007

# Review of material properties, past experiences, procedures, issues and results for a possible solder filled cable as Plan B conductor for the EFDA dipole magnet (Draft Vs 1)

P. Bauer, P. Bruzzone, A. Portone, F. Roth,
M. Vogel, A. Vostner, K. Weiss

ISSN 0458-5895

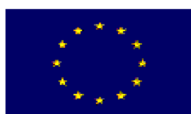

EFDA

European Fusion Development Agreement
Close Support Unit - Garching

# DRAFT Vs 1
# Review of Material Properties, Past Experiences, Procedures, Issues and Results for a Possible Solder Filled Cable as Plan B Conductor for the EFDA Dipole Magnet

**P. Bauer[1], P. Bruzzone[2], A. Portone[1], F. Roth[2], M. Vogel[2], A. Vostner[1], K. Weiss[3]**
**1 ... EFDA, Garching, Germany, 2 ... CRPP, PSI Villigen, Switzerland, 3 ... FZK Karlsruhe**

**March 28th 2007**

1) INTRODUCTION ....................................2

2) PAST EXPERIENCE ....................................5

2.1) Iter Prototype Soldered Cable "NFS"[5] .................................... 5

2.2) "Flat" Cable (or "Plan B") Proposal .................................... 6

3) SOLDER PROPERTIES AND FILLING PROCESS ....................................8

3.1) Choosing the Solder .................................... 8

3.2) The Soldering Process .................................... 11

3.2.1) Soldering Test 1 .................................... 12

3.2.1) Solder-filling of PITSAM II .................................... 13

3.3) Properties of Soldered Cable .................................... 16

3.3.1) Mechanical Testing at Cryogenic Temperatures at FZK .................................... 16

3.3.2) Mechanical Properties of Bi50Sn50 Solder .................................... 17

3.3.3) Mechanical Properties of Bi50Sn50 Soldered Cable with Jacket – Axial Case .................................... 18

3.3.4) Mechanical Properties of Bi50Sn50 Soldered Cable with Jacket – Transverse Case .................................... 19

4) DISCUSSION OF POTENTIAL ISSUES IN A EFDA DIPOLE WITH SOLDERED CABLE ....................................20

4.1) Estimate of AC Loss in the Soldered EFDA High Field Dipole Conductor .................................... 20

4.2) Thermal Simulation of the EFDA Dipole with Soldered Cable .................................... 21

4.3) Mechanical Simulation of the EFDA Dipole with Soldered Cable .................................... 24

5) APPENDIX ....................................26

5.1) Solder companies contacted .................................... 26

## 1) Introduction

The first prototype cables for the superconducting EFDA dipole, SUBSAM I and SUBSAM II, revealed an unexpected degradation of their critical current, $I_c$, in the SULTAN cable test facility. SUBSAM I is the cable sample that is representative of the high field region of the EFDA dipole, while SUBSAM II is the sample representative of the conductor in the low field region of this magnet (in its version 11 configuration). The degradation was clearly correlated with the electromagnetic loading and increased with each loading cycle. The strong Lorentz-forces during testing (i.e. >200 kN/m in the SUBSAM I sample) as well as operation are thought to be responsible for this degradation. The result was surprising, however, since an earlier prototype cable (the so called "Preprototype") performed without such degradation. The difference, however, was that the Preprototype used a lower $J_c$ superconductor and would thus not be suitable for the current EFDA dipole design. With its rectangular cross-section and low void fraction it also used a different conductor design. The Preprototype as well as the coil A conductor in the 45 T hybrid at the NHMFL/Tallahassee/USA perform(ed) under comparable Lorentz-forces as the cables in the EFDA dipole and we therefore hope that a working design for the EFDA dipole can be found quickly[1]. As a alternate option, however, we also pursued a alternate remedy for the Lorentz-force degradation in the EFDA dipole cable. This solution consists of solder filling the conductor. This report summarizes the investigations conducted in preparation for a proposal of a solder filled option of the dipole conductor.

Figure 1 shows an example of an EFDA dipole prototype high field region cable, consisting of 144 Cr coated superconducting $Nb_3Sn$/Cu strands, wound in a 3x3x4x4 pattern (with pitches 58/95/139/213 mm) and compacted into a 1.6 mm wall-thickness stainless steel tube to a void fraction of ~35%. The superconducting strands used in the cable are multi-filamentary $Nb_3Sn$(ternary)/Cu with a critical current density ($J_c$~2300 A/mm$^2$ @ 12T, 4.2 K, zero strain). A layout of this 0.81 mm diameter internal tin (RRP type) strand from OST is shown in the right part of Figure 1. The size of the sub-element (total number 91), and thus the effective filament diameter, is ~80 μm.

A comparative analysis was performed to understand any possible issues in the EFDA cable design. The comparison consisted of benchmarking the EFDA dipole conductor to other state of

**Figure 1: Example of a prototype for the EFDA dipole high field cable. Left: jacket dimensions, Middle: photo during jacketing (photo taken is from a similar but not identical conductor), Right: strand.**

[1] As we are preparing this note a solution has indeed been found in the form of a conductor resembling the pre-prototype conductor, i.e. with a high aspect ratio rectangular cross-section and a low void fraction.

the art fusion cables using a set of parameters related to Lorentzforce effects. These benchmark parameters were the bending strain and the contact pressure under the nominal Lorentzforce loads per strand as proposed by A. Nijhuis[2]. According to Nijhuis the bending strain, $\varepsilon_b$, for a strand under a transverse load $F$ with unsupported length $l$ is given with:

$$\varepsilon_b = \frac{F\ell}{8E_{II}W_b} = \left| W_b = \frac{\pi d^3}{32} \right| \Rightarrow \frac{4F\ell}{E_{II}\pi d^3} \propto \frac{F}{d^3}, \qquad (1)$$

where $F$ is the integrated force over this length (assuming uniform distribution), $E_{II}$ the axial modulus and $d$ the strand diameter.

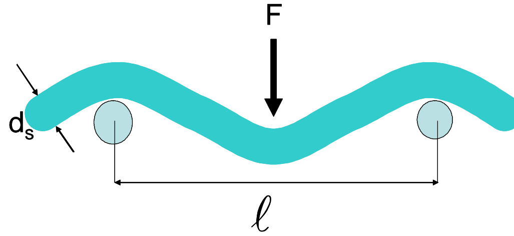


**Figure 2: Illustration of Eq. (1).**

Again according to Nijhuis the peak contact pressure, $\sigma_c$, in a conductor with a square conduit can be estimated with:

$$\sigma_c = \frac{I_s B\sqrt{N}\ell \sin\phi}{d^2} \Rightarrow \propto \frac{I_s B\sqrt{N}}{d^2}, \qquad (2)$$

where $l$ is again the unsupported length, $\phi$ the strand-to-strand angle, $N$, the total number of strands and $I_s$, the current per superconducting strand.

Table 1 compares the load per (superconducting) strand, $F_s = I_s Bl$, and ensuing bending strain and contact pressure for the EFDA dipole cables (including the pre-prototype cable[3]) to those in some state of the art fusion cables, such as the 45 T hybrid[4], the Toroidal Field Model Coil (TFMC[5]) and the "New Full Size" conductor (NFS[6]), a soldered cable prototype developed by CRPP. All these conductors (except that for TFMC) performed, as far as we know, at the expected limits and did not show a significant degradation with loading (some where not submitted to cyclic loading,

[2] A. Nijhuis et al., "Transverse Load Optimization in Nb3Sn CICC Design; Influence of Cabling, Void Fraction and Strand Stiffness", Superconductor Science Technol., 21, 04/2006

[3] P. Bruzzone et al., "Test Results of a Small Size CICC with Advanced Nb3Sn Strands", IEEE Transactions on Applied Superconductivity, Volume 16, Issue 2, June 2006 Page(s):894 - 897

[4] J.R. Miller, "The NHMFL 45-T Hybrid Magnet System: Past, Present and Future", IEEE Transactions on Applied Superconductivity Vol. 13, No. 2, p. 1385 June 2003

[5] J. L. Duchateau et al., ¨Exploring the limits of a very large Nb3Sn conductor: the 80 kA conductor of the International Thermonuclear Experimental Reactor toroidal field model coil.", Superconductor Science and Technology 17 (2004) S241-249

[6] P. Bruzzone et al., "An Alternative CICC Design Aimed at Understanding Critical Performance Issues in $Nb_3Sn$ Conductors for ITER", IEEE Transactions on Applied Superconductivity Vol. 14, No. 2, p. 1527 June 2004

however) such as the prototype cables for the dipole conductor. Note that the benchmark parameters are given relative to the EFDA dipole high field conductor (as shown in Figure 1). This removes any ambiguities regarding the validity of the formula and of the input parameters other than force and jacket geometry. The table shows that the forces per strand are considerably higher in the EFDA dipole designs than in the 45 T hybrid or the TFMC. Those larger forces, however, do not necessarily translate into worse bending strain or contact pressure. In the case of the hybrid, for instance, this is the result of the smaller hybrid strand diameter, giving a larger deflection for a smaller force. The TFMC cable is much larger, which increases the contact pressure accordingly. Interestingly, the soldered NFS conductor went to conditions beyond those of the high field cable and performed well. The example of the NFS conductor is essentially the reason why we hope to cure the cable degradation with soldering. Also note that the pre-prototype EFDA dipole high field cable performed so well that it could be operated at force levels exceeding those of the current cable design, and that without solder filling.

As a possible remedy to the $I_c$ degradation in the EFDA dipole cable, a solder filled version of these cables was developed. This note discussed the experience gained in this process and discusses the potential issues of the solder filling concept. As a first step we will review past experiences with soldered cable designs.

**Table 1: Comparing Lorentz-loads in the EFDA dipole and in state of the art fusion magnet conductors.**

| | **B/I (T/ kA)** | **$N_{sc}$ / $N_{Cu}$** | **$F_s$ (kN/ m)** | **d (mm)** | **$\varepsilon_{b,r}$ [1]** | **Outer jacket dim[2] (mm)** | **$P_{ave}$ (MPa)** | **$P_{c,r}$ [3] (MPa)** | **VF (%)** | **Comment** |
|---|---|---|---|---|---|---|---|---|---|---|
| EFDA Dipole (HF1) | 12.5/ 17.5 | 144/0 | 1.52 | 0.81 | 1 | 15.8/13.2 (1.65) | 17.5 | 1 | 35 | design, 1st prototype failed |
| EFDA Dipole (LF2) | 6.5/ 17.5 | 36/72 | 3.16 | 0.81 | 2.1 | 12.7/12.6 (1.5) | 11.7 | 1.8 | 35 | design, 1st prototype failed |
| EFDA Dipole (PreProto[4]) | 9/25 | 84/24 | 2.68 | 0.81 | 1.76 | 18.4/7.7 (1.0) | 13.7 | 1.5[5] | 28 | performed as expected |
| NHMFL 45T hybrid coil A | 15.7/ 10 | 450/ 75 | 0.35 | 0.433 | 1.51 | 16.2/13.7 1 (1.64) | 12.2 | 1.5[6] | 37 | |
| NFS[7] (soldered, B) | 11/ 56 | 588/ 924 | 1.05 | 0.7 | 1.1 | 36.4 Ø (2.25) | 29[8] | 4.5[9,11] | 37 | solid cooling tube, no degradation (while non-soldered version was degraded) |
| TFMC | 10/ 80 | 720/ 360 | 1.1 | 0.81 | 0.73 | 40.7 Ø (1.6) | 32[8] | 3[10,11] | 36 | cooling spiral, degradation observed |

1) Strand bending strain, relative to the EFDA Dipole HF1 conductor case using Equ. 1.
2) Outer dimension (larger dimension assumed to react forces).
3) Contact pressure, relative to the EFDA Dipole HF1 conductor case using Equ. 2. Assumes square jacket and neglects differences in cabling pattern, twist pitches, ..etc
4) Test results.
5) Due to the large aspect ratio (~3) of the cable the approximation Equ. (2) overestimates the contact pressure for this cable.
6) It was not clarified how Equ. 2 applies to the particular cabling pattern (septuplet primary stage) and the much larger diameter of the Cu strands, which characterize this particular cable.
7) Test result for highest Lorentz-force load.
8) The jacket inner diameter and a factor 1.5 were used to calculate the pressure in the circular geometry.
9) Central cooling tube, braided nature of cable as well as round cross-sectional deviate strongly from assumptions leading to Equ. 2.
10) Central cooling channel and SS foil around petals are not taken into account in the model leading to Equ. 2
11) Equ. 2 was multiplied by 1.5 in the calculation of the peak contact stress to take into account the enhancement of stresses in the round geometry

## 2) Past Experience

There are several examples of soldered conductors used in fusion magnets. Some of them are shown in Figure 3. In some cases the superconductor was $Nb_3Sn$, so the experience is indeed relevant to our case. The largest scale application to date was the CH coil for the Large Coil Task project[7], where a NbTi (0.46 mm) multi-stage (10(+1Cu) x 6(+1Cu) x 8) cable was pulled through a CdZnAg solder and then cabled in the soldered form. This cable had no jacket and a solder with high mechanical strength (290 MPa yield, 80 MPa shear) was therefore needed. A Cu cooling tube in the center provided the liquid helium cooling. The coil performed at the nominal 8T, but had stability issues. Two more recent examples will be discussed in further detail since the information was easy to collect. The first is the so-called "NFS" conductor and the second the "flat" conductor as recently developed at CRPP as plan B for the ITER project.

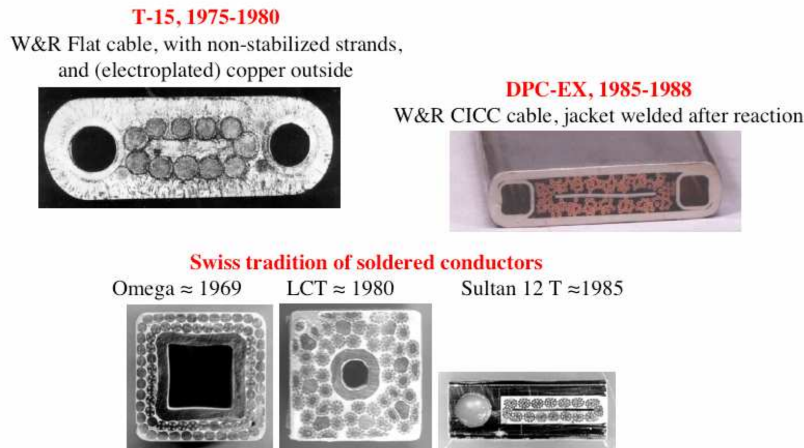


**Figure 3: A collection of soldered conductors for fusion magnets. Courtesy of P. Bruzzone.**

### 2.1) Iter Prototype Soldered Cable "NFS"[5]

The "New Full Size" conductor was intended as an alternative design for the ITER TF conductor, which suffers from (apparently) similar, although much less severe, performance degradation problems as the EFDA dipole conductor. The cable was therefore designed to meet the ITER TF coil conductor specification. The alternate design concept of this special cable was the use of In50Pb50 solder (Indalloy7™, liquidus 215°C) to stabilize the braided conductor as well as a central cooling tube for indirect cooling with supercritical helium. As shown in Figure 4, the Ti jacket is round with a 36.4 mm diameter (2.5 mm thick wall). Also the central cooling channel (8x6) is made of Ti. The cable was "braided" at VNIIKP in the primary stage (14 SC + 15

[7] "The Large Coil Task Report", Fusion Engineering and Design, Vol 7, 1988

[5] P. Bruzzone et al., "An Alternative CICC Design Aimed at Understanding Critical Performance Issues in $Nb_3Sn$ Conductors for ITER", IEEE Transactions on Applied Superconductivity Vol. 14, No. 2, p. 1527 June 2004

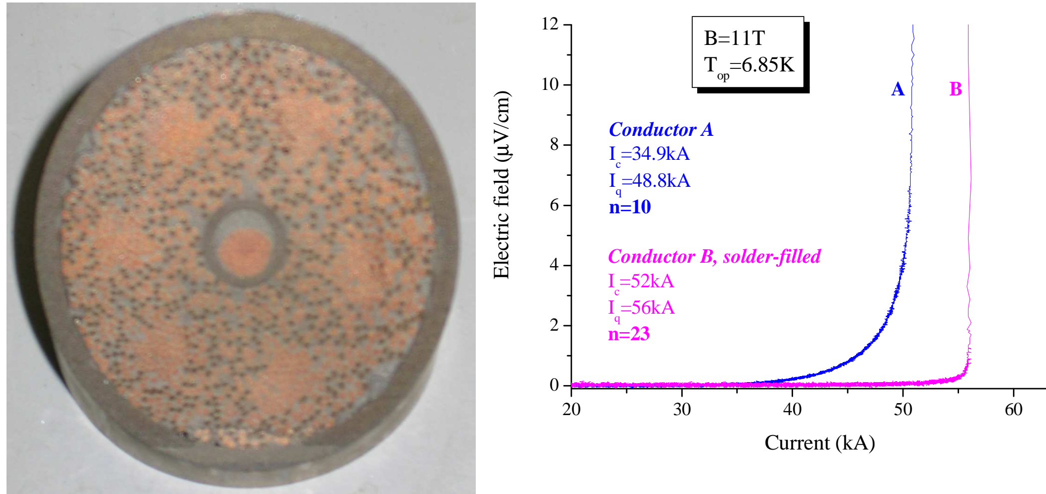


**Figure 4: The CRPP NFS conductor and test results.**

Cu strands), giving a total of 588 superconducting (diameter 0.7 mm) and 924 Cu strands (49+(29x7))x6, pitches: 380/160/390 mm) with a 37% void fraction. The solder filled leg used strands that were not Cr coated. The self-mixed solder was filled into the conductor after the heat treatment. The soldered cable performed close to expectation (assuming ε=-0.45% after cool-down). Interestingly the non-soldered leg was degraded (Figure 4). It is not clear if current e-distribution was facilitated after removal of the Cr coating on the strands. It is not unlikely, however, that mechanical stabilization provided by the solder played a major role in the performance improvement of the soldered leg. No cycling tests were performed.

## 2.2) “Flat” Cable (or “Plan B”) Proposal[8]

The “flat” cable is the most recent alternative fusion magnet conductor concept developed at CRPP (Figure 5). The cable uses a Wind-and-React approach and therefore requires solder to protect the brittle strands during the magnet winding procedure. Furthermore it uses high $J_c$ strands in a cable pattern that is very similar to the Rutherford cables in accelerator magnets, which achieve very high packing factors, further enhancing the mechanical stabilization of the strands. A first prototype of this cable was successfully tested and achieved the expected $I_c$, if assuming $\varepsilon=-0.28\%$ compressive strain. The solder chosen was Bi58Sn42, a lead-free solder with a low melting point and high resistivity. Further discussion of the solder is given in section 3. Tests results for the flat cable prototype as compared to expectation (“calculated”) are shown in Figure 6. Note, however, that a recent test showed, that the non-soldered version of this conductor achieved similar, “as-expected” performance.

[8] P. Bruzzone et al., “Test Results of a Large Size, Forced Flow Nb3Sn Conductor, Based on a Design Alternative to the Cable in Conduit”, Preprint, Applied Superconductivity Conference, Aug. 2006, Seattle, USA

After heat treatment, the two bent sections are straightened, encased in the jacket and filled with SnBi low melting alloy (185 C)

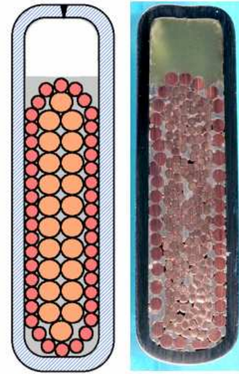

Cable filled by SnBi alloy,
$\rho$ = 6.55 $10^{-8}$ Ωm
He ≈ 100 $mm^2$
Welded steel jacket, 16.3 x 53.5 mm

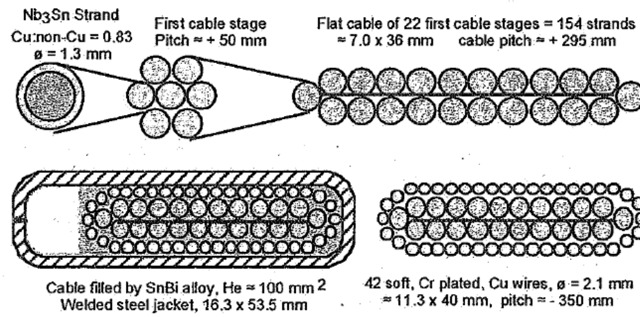


**Figure 5: The “flat” cable developed by CRPP.**

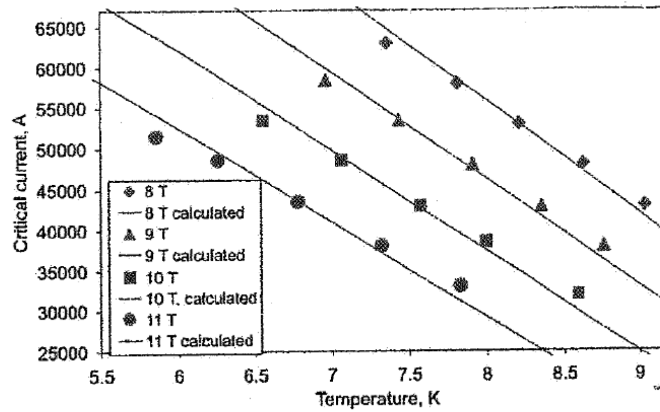


Fig. 3 Summary of dc results and calculated performance with ε = -0.28% and $k_{eff} = 4 \cdot 10^{-2}$ T/kA

**Figure 6: Test result flat cable prototype 1.**

## 3) Solder Properties and Filling Process

### 3.1) Choosing the Solder

The main properties of the solder to be used for the impregnation of the EFDA dipole cable are listed below. Obviously, some of the requirements are contradictory and compromises need to be made.

- The solder filling process is supposed to take place after the coil reaction and impregnation process. To prevent significant softening of the coil impregnation and the epoxy polymerization temperature being ~165°C, the liquidus temperature needs to therefore be below 160°C. The low melting point also prevents the diffusion of the Sn into the Cu. Since the magnet fabrication procedure foresees a second epoxy impregnation after the solder filling (this time of the entire coil assembly, including yoke and shrinking cylinder) the solidus temperature needs to remain above 150°C to allow for a second epoxy impregnation at ~135°C.
- Low viscosity in the liquid state to favour a fast impregnation.
- High electrical resistivity (and NO superconductivity!) to reduce AC losses.
- "Matched" thermal contraction to prevent separation from the cable and conduit after cool-down.
- High yield strength and modulus to provide mechanical support to the strands.
- Low yield strength and modulus to reduce the transfer of cumulative magnet load from the jacket to the cable during operation.
- High thermal conductivity to improve cable thermal stability.

The following discusses a selection of different solder types and compares their properties as basis for the choice of solder for the EFDA dipole conductor. Assuming a typical density of 8370 kg/m$^3$ and a cable volume of 12.6 x 9.7 = 122.2 mm$^2$ per m of conductor, as well as a void fraction of 35%, the amount of solder needed for 1m of cable is 0.31 kg. A sample for Sultan (~6 m) therefore requires ~2 kg. A total double layer of the EFDA dipole with 120 m requires ~40 kg. With 8 double-layers per pole, the total solder requirement for the EFDA dipole would be ~640 kg.

**The following tables (**

**Table 2-**

Table 3) summarize the properties of different solder types as far as the data could be obtained. These are: -1- Sn63Pb37 (eutectic), the standard solder which is best known, -2- Bi58Sn42 (eutectic), the solder chosen by CRPP for the flat cable samples, -3- Bi50Sn50, our choice of solder and -4- Pb50In50 (Indalloy7™), the solder chosen by CRPP for the NFS sample. The properties of the solders can sometimes be better understood on the basis of the elements they are composed from. There are therefore also tables (

Table 4 -

Table 5) with the properties of the compositional elements.

The Bi-Sn solder is Pb free and thus environmentally less problematic. It is also much less costly than solders containing In. Its biggest advantage, however, is its low melting point and high

electrical resistivity, both consequences of the presence of Bi. The thermal shrinkage is also more moderate than in standard PbSn material. The change of density at the phase transition is small compared to the standard solder, another advantage. This is the result of the Bi density increasing upon melting (3.35%)[9]. The Bi-Sn solder is relatively strong (though slightly softer than PbSn)

**Table 2: Sn63Pb37, Bi58Sn42, Bi50Sn50 and Pb50In50: Physical and Thermal Properties at room-temperature. Sources: NIST Solder Property Handbook 2002, Thermophysical Properties of Matter – the TPRC Series, IFI Plenum 1970.**

| | **Sn63Pb37 eutectic** | **Bi58Sn42 eutectic** | **Bi50Sn50** | **Pb50In50 Indalloy7** |
|---|---|---|---|---|
| Density (sol/liqu) ($g/cm^3$) | 8.42/? | 8.56/? | 8.37/? | 8.86/? |
| Cost ($/kg)<br>Young's Modulus (GPa)<br>Yield Strength (MPa)<br>Shear Strength (MPa) | 3.8-5.2<br>15.7-35<br>27.2-43<br>28.4-37 | 7.57<br>11.9<br>49.1<br>34-48 | <br><br>57<br> | <br><br>32.2[2]<br>18.5 |
| Electrical Resistivity (μΩ·cm) | 14.5-17 | 38 | | 29 |
| Melting point (°C) | 183 | 138 | 152 (liquidus) | 184-210 |
| Volume Change during Melting (%) | 4 | 0.77 | | |
| Thermal Conductivity (W/(m·K))<br>Specific Heat (J/(kg·K))<br><br>Viscosity in liquid state (Pa-s)<br>Thermal Expansion ($10^{-6}$/K) | 50.9<br>190.4<br><br>0.00224[3]<br>24-25 | 19<br>176.3<br><br><br>14.3-15 | 33<br>probably same as in 58/40<br><br>18.6 | 22<br><br><br><br>27 |
| Comment | standard reference, cheap | established, inexpensive, used for flat cable at CRPP | candidate for EFDA dipole plan B | expensive, used for NFS at CRPP |

1) 0.5% yield strength
2) Ultimate strength
3) The viscosity of water is 0.0009 Pa-s, Propanol has 0.002 Pa-s.

**Table 3: Sn63Pb37, Bi58Sn42, Bi50Sn50 and Pb50In50: Physical and Thermal Properties at very low temperatures. Sources: NIST Solder Property Handbook 2002, Thermophysical Properties of Matter – the TPRC Series, IFI Plenum 1970.**

| | **Sn63Pb37 eutectic** | **Bi58Sn42 eutectic** | **Bi50Sn50** | **Pb50In50 Indalloy7** |
|---|---|---|---|---|
| Density ($g/cm^3$)<br>Young's Modulus (GPa)<br>Yield Strength (MPa)<br>Shear Strength (MPa) | | | <br>~60[3]<br>~25[3]<br> | |
| Electrical Resistivity (μΩ·cm) | | 6.55[2] | | |
| Thermal Conductivity (W/(m·K))<br><br>Specific Heat (J/(kg·K))<br><br>Therm Contract ($\Delta L(300K\text{-}4K)/L_0(300K)$) | 10<br><br>0.63<br><br>0.2[1] | 17<br>(Bi70Sn30@40K)<br>0.33<br>(Bi9Sn91)<br>na | | 0.9<br>(Pb64.4In35.6)<br>na<br><br>na |

[9] F. Hua et al., "Eutectic SnBi as an alternative to Pb free solders", Journal on the Properties of Electronic Components, 1998 Electronic Components and Technology Conference??

| (%) | | | | | |
|---|---|---|---|---|---|

1) NASA data = questionable – too low contraction compared to elemental data and extrapolation from RT α
2) Measurement at CRPP (published for instance in P. Bruzzone's ASC 06 paper titled: "Test Results of a Large Size, Forced Flow Nb3Sn Conductor, Based on a Design Alternative to the Cable-in-Conduit")
3) Measurement by K. Weiss, FZK, see discussion in section 3.3).

**Table 4: Pure Copper, Tin, Lead, Indium and Bismuth: Physical and Thermal Properties at room temperature. Sources: NIST Solder Property Handbook 2002, Thermophysical Properties of Matter – the TPRC Series, IFI Plenum 1970.**

| | Cu | Sn | Pb | In | Bi |
|---|---|---|---|---|---|
| Density ($g/cm^3$) | 8.9 | 7.3 | 11.34 | 7.3 | 9.8 |
| Cost ($/kg) | 1.5 | 7.7 | 1 | 275 | 7.5 |
| Young's Modulus (GPa) | 117-130 | 41-45 | 17.9 | 10.5 | 32 |
| Yield Strength (MPa) | 340 | 25 | 9.5[1] | | |
| Shear Strength (MPa) | | 22.6 | | 6.1 | |
| Electrical Resistivity (μΩ·cm) | 1.7 | 11.5 | 19.3 | 8.0 | 115 |
| Melting point (°C)) | 1083 | 232 | 327 | 156.4 | 271 |
| Thermal Conductivity (W/(m·K)) | 398-416 | 67-73 | 35 | 82 | 8-11.2 |
| Specific Heat (J/(kg·K)) | 385 | 227 | 129 | 239 | 122 |
| Thermal Expansion ($10^{-6}$/K) | 16.9-17.1 | 21-23 | 29.1 | 32.1 | 13.4 |

1) 0.5% yield strength

**Table 5: Pure Copper, Tin, Lead, Indium and Bismuth: Physical and Thermal Properties at low temperature. Sources: NIST Solder Property Handbook 2002, Thermophysical Properties of Matter – the TPRC Series, IFI Plenum 1970.**

| | Cu | Sn | Pb | In | Bi |
|---|---|---|---|---|---|
| Density ($g/cm^3$) | | | | | |
| Young's Modulus (GPa) | | | | | |
| Yield Strength (MPa) | | | | | |
| Shear Strength (MPa) | | | | | |
| Electrical Resistivity (μΩ·cm) | RRR 100: $1.7 \cdot 10^{-2}$ | | | | |
| Thermal Conductivity[1] (W/(m·K)) | $10^2$-$10^4$ | $2 \cdot 10^2$-$2 \cdot 10^4$ | $10^2$-$2 \cdot 10^3$ | $10^2$-$4 \cdot 10^3$ | $2 \cdot 10^2$-$1.5 \cdot 10^3$ |
| Specific Heat (J/(kg·K)) | 17 | 0.3 | 1.4 | 1.1 | 1.1 |
| Therm Contract ($\Delta L(300K\text{-}4K)/L_0(300K)$) (%) | 0.3 | 0.47 | 0.7 | 0.7 | 0.34 |

1) Upper bounds of thermal conductivity only for high purity, annealed material – Lower bound recommended for low purity and/or alloying

and brittle. Its fatigue life is poorer than that of PbSn, especially when slightly contaminated or in contact with Pb[10]. The microstructure of the Bi58Sn42 solder is shown in Figure 7[8]. The lamellas are typical for eutectics. The Bi solders were also proven to work at cryogenic temperatures, not only by CRPP. The viscosity of solders is typically low, approximately twice that of water.

A variant of the Bi-Sn solder, Bi50Sn50 was chosen for the EFDA dipole alternate conductor, because its liquidus temperature is close to the desired value. The liquidus temperatures can be further fine-tuned, as can be seen in the phase-diagram shown in Figure 8. The price to pay for

[10] Mei et al., "Low Temperature Solders", Hewlett Packard Journal, Aug. 1996

chosing a mixture with less Bi than the eutectic is a slight decrease in electrical resistivity and a slight increase in thermal shrinkage. Assuming a 30% solder fraction and a Cu/NCu ratio of 1, one obtains an average (over 300K-0K) contraction coefficient of 10.5 ppm/ºK for the Bi50Sn50-strand composite. This is close to that of the steel jacket (~9 ppm/ºK). The solder and conductor will not shrink at the same rate, however, since the solder has a low yield strength. The reduced thermal shrinkage of the solder prevents the hydrostatic pressure to rise strongly in the cable. Another advantage of the 50/50 BiSn mixture is its higher thermal conductivity (than for the eutectic).

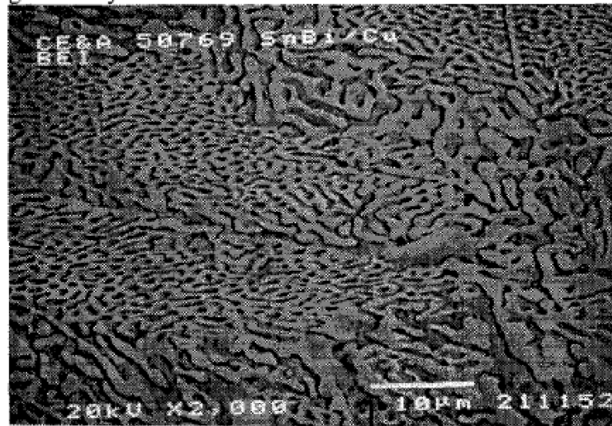


**Figure 7: Microstructure and phase-diagram of Bi58Sn42 solder.**

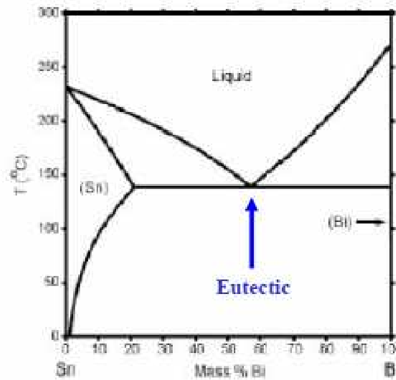


**Figure 8: Phase-diagram of Bi-Sn solder.**

## 3.2) The Soldering Process

The main complications for the solder-filling process in the EFDA dipole are:

- The minimum batch length of ~120 m (one double layer) and the associated filling issues.
- The two-step epoxy impregnation and related interferences due to epoxy polymerization.
- Possible interference with joint brazing.
- Possible tin diffusion into the strand.

The following discusses the experimental work performed at CRPP to address the above issues. The most important activity consisted in the preparation of a SULTAN sample of a solder-filled EFDA dipole prototype conductor (called PITSAM II). The solder-filling of this conductor was

preceded by a solder-filling test of the previously tested dipole high-field conductor prototype (SUBSAM I) that had given a strongly degraded test performance. The lessons learned in the first solder filling campaign were applied to the second solder filling campaign.

3.2.1) Soldering Test 1

Soldering test 1 was performed at CRPP-Villigen on 10/20/06 under EFDA supervision on the previously tested EFDA dipole high field 1 conductor (so-called SUBSAM I). The sample was filled with a remaining batch of eutectic BiSn solder (i.e. not the exact solder mixture foreseen for the case of the EFDA dipole. The procedure consisted of the following steps:

- Mounted solder bars into reservoir, closed (welded) and weighed reservoir;
- Leak-checked system;
- Tested diagnostic systems (temp sensors, pressure gauges, solder filling indicators*)
- Transferred system into tube furnace;
- Started furnace, started pump (both reservoir and end of solder filling line);
- Set furnace to T~20°C above liquidus temperature (138°C);
- Measured start and end of solder-filling (could not be performed in this test);
- Withdrew assembly from furnace;
- Weighed reservoir to estimate quantity of solder dispensed;
- Cut conductor for inspection and sample preparation;

The test setup is shown in Figure 9. Figure 10 shows some pictures of the soldering test 1 setup.

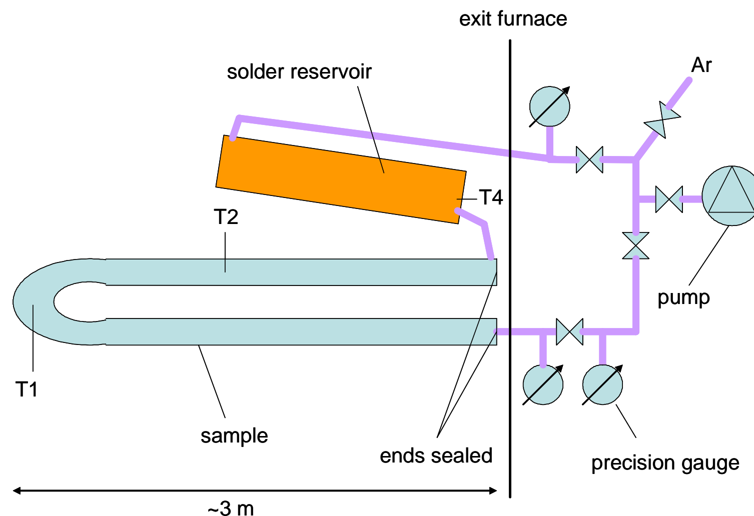


**Figure 9: Schematic of solder filling test. Temp sensors are thermo-couples; Pressure gauges are mostly low precision with the exception of a Pirani gauge;**

The first soldering test was successful, but not without difficulties. The lack of diagnostics to measure the start and end of the solder filling process complicated the task considerably. Time constraints also required the increase of the furnace temperature to slightly above 200°C to accelerate the melting of the solder. The furnace run was started at 14:25 and at 15:46 the furnace reached 200°C (T1: 175.6°C, T4: 157.3°C). The temperature was allowed to increase further until at 16:11 (T1: 216.9°C, T4: 172.6°C) when the “melt-test” finally was positive. The melt-test, an improvised method, consisted of sending a pressure wave through the evacuated sample from the

solder reservoir side of the sample. When the pressure wave did not appear at the pressure gauges at the end of the sample the conclusion was drawn that the conductor was (at least in one section) completely filled with solder. The sample was opened and inspected as well as a tensile test

**Figure 10: Top left: Solder test assembly before insertion into furnace. Top right: Solder reservoir with pumping port. Bottom left: (top) and outlet (bottom) into cable sample. On the right side are the sealed joints., Bottom middle: Plumbing: bottom: pumping port; Right: Line to Argon. Setup shown does not correspond exactly to final version as shown in schematic. Bottom right: Complete assembly mounted into furnace.**

**Figure 11: Left: Partially melted solder bars. Right: Result of solder-filling of SUBSAM I cable.**

sample cut from it. The result of solder-filling the SUBSAM I conductor is shown in Figure 11. The filling process appears to be complete. Weighing of the reservoir before and after soldering reveals that 1.8 kg of solder were distributed into the conductor, very close to the estimated value needed for filling the 6 m long sample (estimate: 0.31 kg/m). The remaining solder removed from the reservoir had not been completely melted in the process. The solder filling test also gave some information on the solder wetting of the strand inside the cable. Opening of the conductor after soldering test 1 revealed that the solder was only loosely bonded to the Cr coated strands, i.e. acting more as filler than tightly bonding.

3.2.1) Solder-filling of PITSAM II

The lessons learned in soldering test 1 were applied to the solder filling of PITSAM II on Nov. 7th 2006. These are listed in the following and also shown in Figure 12 and Figure 13. The PITSAM II conductor was the so-called low-field I conductor from the first wave of EFDA dipole prototype cables. The salient features of its design are: 48 Nb3Sn/Cu strands (60 Cu strands) in a (3x3)x3x4 cable in a 12.63x12.62 mm square steel jacket (1.5 mm thickness). Unlike soldering test 1 the PITSAM II sample was filled with the Bi50Sn50 solder (liquidus 152ºC) chosen for the solder filling option of the EFDA dipole:

- The filling time needed to be measured and the filling process had to be monitored. Therefore a siphon was installed behind the reservoir to prevent premature dripping of melted solder into the cable. The filling process could be launched deliberately via the pressurization of the reservoir, which pushed the liquid through the siphon. An additional valve was placed between the pump and the reservoir, allowing pressurization of the reservoir, while pumping on the back end of the cable. This requires that the pump be isolated from the Ar supply. In addition the set-up included solder-filling sensors, using a simple design developed at CRPP. The sensors consisted of pairs of thermo-couple wires, with one end installed inside the cable and the other connected to the conduit wall. The solder short-contacts the two terminations triggering a sound signal in a simple connectivity testing device.
- Then, the system was kept at the filling temperature (<20ºC above the melting point) long enough for the solder to melt. The temperature profiles are shown in Figure 14. To reduce this time the heat transfer into the solder reservoir needed to be improved. This was achieved by pre-melting the BiSn solder and filling into the reservoir, thus increasing the total area of contact between reservoir wall and solder. The conductor was also filled with Ar gas under pressure during the heating in order to further improve the heat transfer.

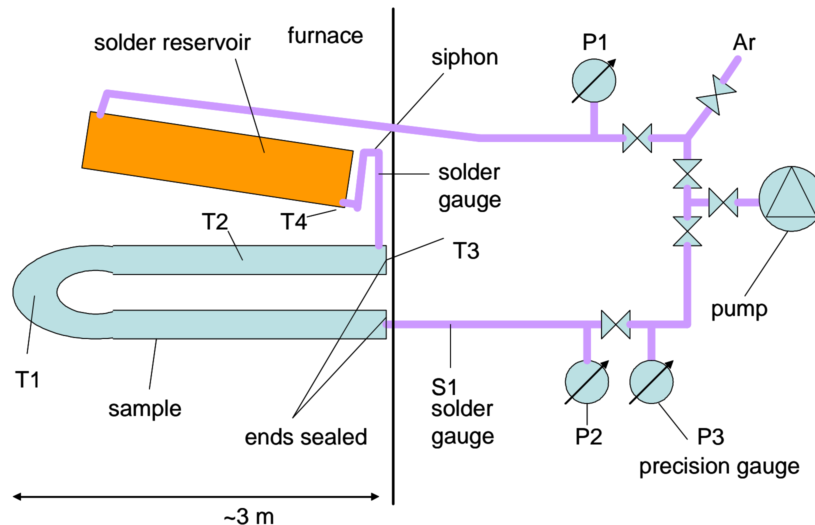


**Figure 12: Schematic of solder filling of PITSAM II. Temp sensors are thermo-couples; Pressure gauges are mostly low precision with the exception of a Pirani gauge.**

The filling of the PITSAM II conductor was successful. The system was kept in the furnace for 7 hours. The conductor pressure was lowered to < 1mbar within a few minutes, just before the reservoir was pressurized to start the solder filling. The solder filling process took 1 min 25 secs, corresponding to a filling velocity of 4.2 m/min. A total of 2 kg of solder was dispensed inside the conductor (including pipes connecting the reservoir to the sample and out of the sample). This is consistent with the expected quantity of solder required to fill the cable voids.

In the context of the testing of the flat cable CRPP performed a test of Cu-Sn reaction at different temperatures. For BiSn solder the reaction depends on temperature, being negligible at T<170ºC.

As an additional improvement for the solder filling of the magnet from the PITSAM II filling it could be useful to use a separate heating system for the solder bath, possibly placed on the outside of the furnace.

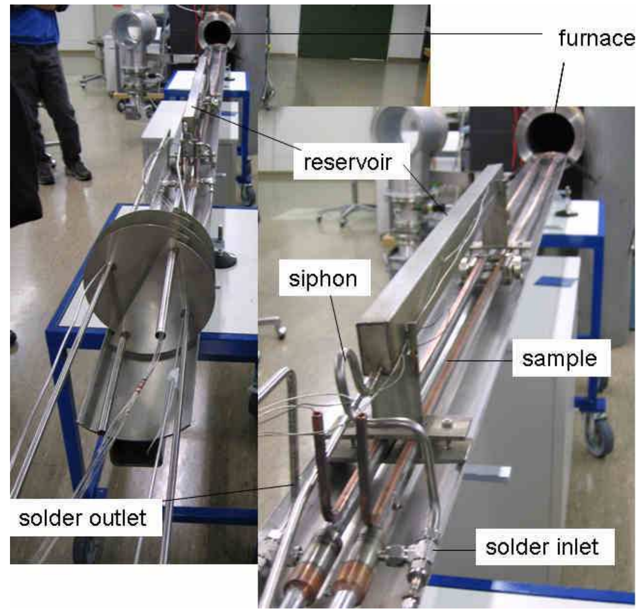


**Figure 13: Soldering setup of the PITSAM II conductor. The improvements to the system consisted of the use of a siphon to prevent premature dripping of melted solder into the cable. In addition the set-up included solder-filling diagnostics.**

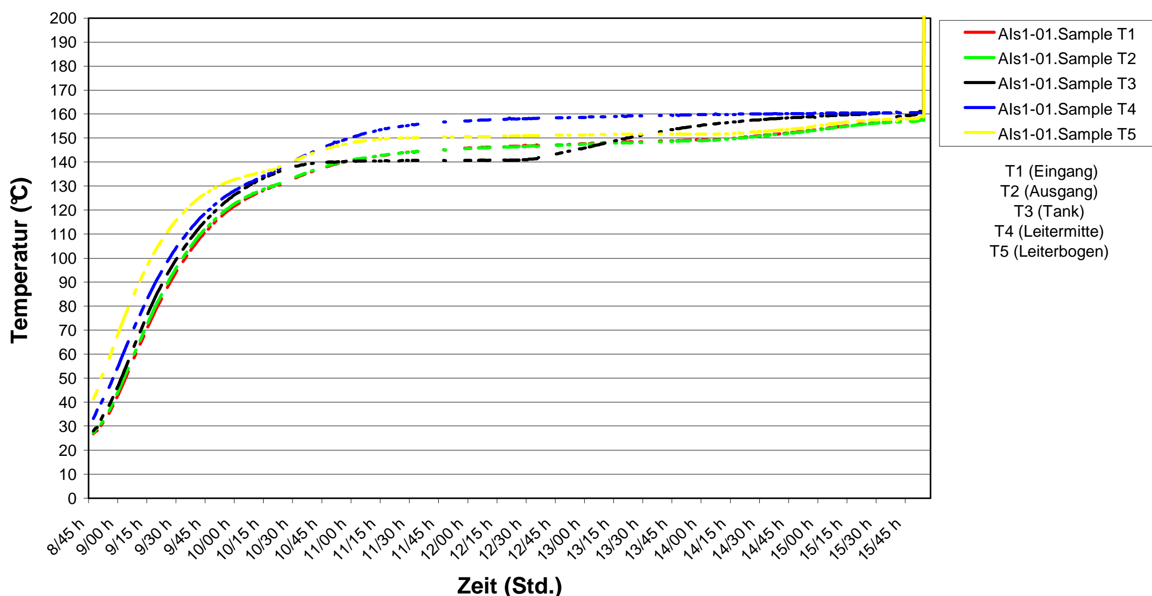


**Figure 14: Temperature sensor readings during PITSAM II solder filling.**

## 3.3) Properties of Soldered Cable

Several issues arise in the EFDA dipole design when using a solder filled cable. Among them is increased mechanical loading of the superconductor due to cumulative forces from other turns (which otherwise would be channelled around the cable through the jacket) and increased thermal pre-compression (and thus related performance reduction) of the superconductor in the conduit. The severity of these effects depend mostly on the mechanical properties of the solder filled cable or the solder itself. In order to understand better the mechanical characteristics of the soldered CICC cable we conducted measurements of the stress-strain characteristics at room and cryogenic temperatures.

### 3.3.1) Mechanical Testing at Cryogenic Temperatures at FZK

The following briefly introduces the FZK facilities used for the mechanical characterization of the solder filled conductor (Figure 15). For measurements on the soldered cable with jacket the cryogenic tensile facility, system Schenck (630 kN) at a working temperature of 4.2 K (LHe), was used. The tests on short solder specimen were performed in the cryogenic MTS (25 kN) tensile test facility, operating between 295 K and 7 K. The strain measurement will be done, using the high sensitive extensometer system developed by ITP/FZK for cryogenic testing.

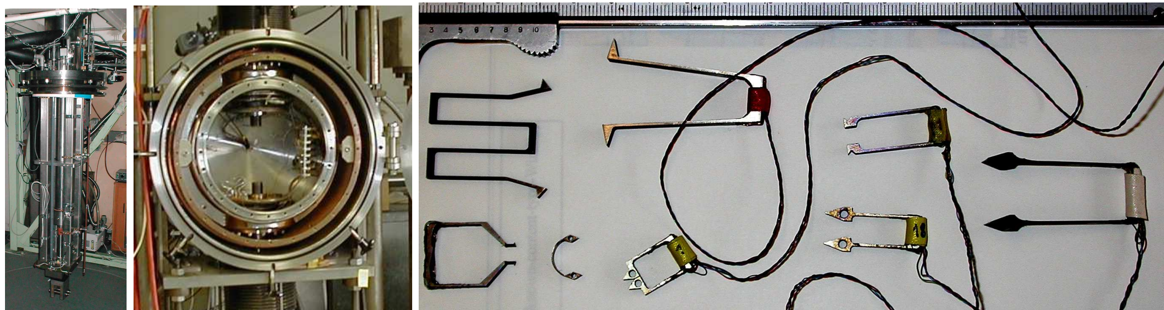

**Figure 15: Cryogenic mechanical testing equipment at FZK. Left: Schenck facility (630 kN), Middle: MTS (25 kN), Right: Extensometers developed at FZK.**

The samples were mounted in tailor-made force grips from hardened steel, as shown in Figure 16. The sample length was determined to be minimum 1 twist pitch (~250 mm) long, plus sample length for mounting of grips (total = 0.5 m). Minimum force of the grips was determined to be ~10 metric tons. The solder sample was threaded at the ends and screwed into an existing mounting system.

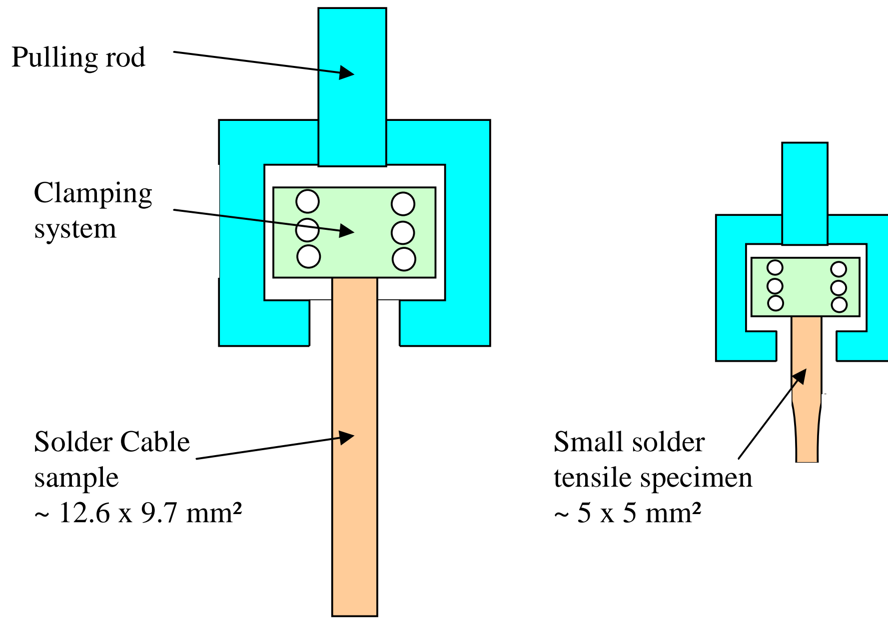


**Figure 16: Sample-holders for FZK mechanical testing.**

3.3.2) Mechanical Properties of Bi50Sn50 Solder

The measurement of the stress-strain characteristic at 7 K revealed the mechanical benchmark data for Bi50Sn50 solder given in Figure 18. The material is very brittle, so only the ultimate strength could be determined. The modulus is ~65 GPa and larger than expected.

**Figure 17: BiSn solder specimen after testing at FZK.**

Results

| Specimen | T [K] | Young Modulus [GPa] | Ultimate Tensile Strength [MPa] | Total El. [%] |
|---|---|---|---|---|
| Lot-1 | 7 | 63,2 | 20,5 | 0,04 |
| Lot-2 | 7 | 55,6 | 26,8 | 0,05 |
| | | | | |

**Figure 18: Results of stress-strain characterization of Bi50Sn50 solder at FZK.**

3.3.3) Mechanical Properties of Bi50Sn50 Soldered Cable with Jacket – Axial Case

The solder filled sample produced in the solder-test 1 at CRPP is shown before testing at 4.2 K in Figure 19 and Figure 20. Although the force grips could not prevent slipping during the experiment the Young modulus and yield strength of the soldered cable could be measured

**Figure 19: Soldered cable sample before testing.**

**Figure 20: Soldered Cable Sample mounted into the test-rig: Left Cryostat insert, Middle: Force grips with sample, Right: Test Insert before insertion in cryostat.**

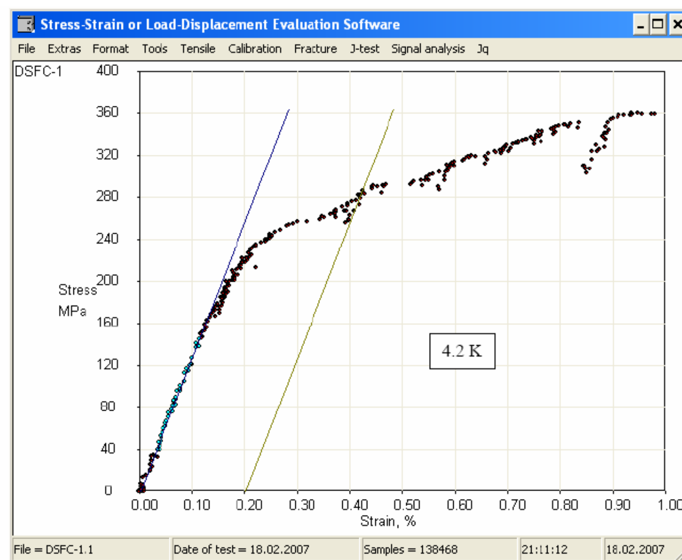


**Figure 21: Stress-strain characteristic of soldered cable at 4.2 K.**

precisely. The experimental result is shown in Figure 21. The Young modulus derived from these experiments is 128 GPa. The yield strength is 282 MPa. A rough analysis indicates that a cable without solder would have an axial modulus of 114 GPa, while the measured value is 128 GPa. This result indicates that the solder has a noticeable effect on the overall mechanical properties of the conductor. The analysis was performed with a simple model that calculates the total modulus of the conductor from the sum of the moduli of the single components weighed with the cross-sectional area fraction of each component. The cross-sectional areas and estimated elastic moduli of the various materials are as indicated in Table 6. The reason why the Cu and bronze modulus needed to be set relatively high is not clear (note that the Cu and Bronze yield in tension during the cool-down of the sample). Possibly the simplified 1 dimensional model under-estimates the effective modulus of the composite.

**Table 6: Data for simple model of cable modulus.**

| Material | A ($mm^2$) | E (GPa) |
|---|---|---|
| Nb3Sn | 24.78 | 100 |
| Cu | 38.72 | 40 |
| Bronze (high tin) | 13.17 | 80 |
| Barrier (Nb) | 0.77 | 110 |
| Steel | 90.42 | 210 |
| Solder | 43.51 | 60 |

### 3.3.4) Mechanical Properties of Bi50Sn50 Soldered Cable with Jacket – Transverse Case

The case that is more relevant for the magnet environment is that of transverse compression. In a non solder-filled cable the jacket is expected to dominate the stress-strain characteristic. In a solder filled cable the content of the jacket (cable plus solder) is expected to play a noticeable role.

A measurement of the transverse stress-strain characteristic is discussed in the following:

DATA ARE MISSING

DERIVE TRANSVERSE MODULUS OF CABLE, COMPARING RESULT OF SOLDER-FILLED CABLE WITH RESULT OF EMPTY JACKET

## 4) Discussion of Potential Issues in a EFDA Dipole with Soldered Cable

The solder filling of the conductor may affect the performance of the dipole in what refers to: AC-losses, reduced cooling / stability and mechanically. These issues are discussed in further detail in the following. All our discussions refer to the version 11 design of the EFDA dipole (Figure 22).

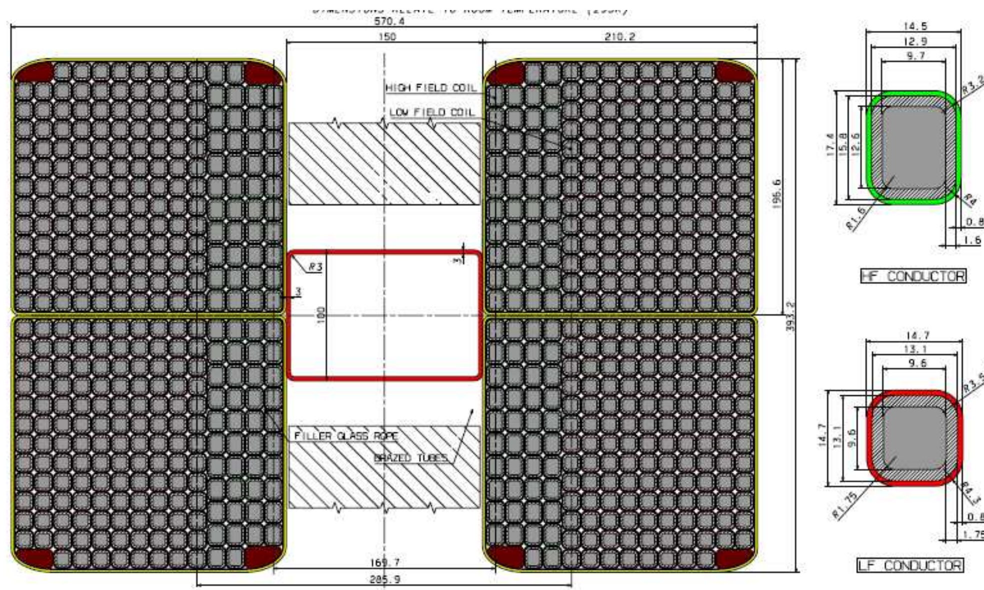


**Figure 22: Version II design of the EFDA dipole winding pack.**

### 4.1) Estimate of AC Loss in the Soldered EFDA High Field Dipole Conductor

The following presents a back of the envelope estimate of the increase in AC loss to be expected in the solder filled cable during operation of the AC coil, as opposed to the non-solder filled cable. The loss time constant $n\tau$ can be estimated for the condition that the cable twist pitch is comparable to the cable transverse dimension (note that this condition is NOT fulfilled in the EFDA dipole cable), with:

$n=1$, $\tau \sim \mu_0/2(L_p/2/\pi)^2 1/\rho$ (sec),

**where $L_p$ is the twist pitch of the last cabling stage ($L_p$ =200 mm, last stage of 3x3x4x4), $\rho=6.6\times10^{-8}$ Ωm, the transverse cable resistivity (in this case the solder resistivity at cryo-temp, see**

Table 3). Using these assumptions we obtain **$\tau$ ~10 msec**! This is 10 times smaller than the experimental data obtained for the soldered flat cable, recently tested at CRPP (Figure 23). Note, however, that the last stage flat cable pitch is 295 mm, which can explain a larger **$\tau$**. Note, however, that the above estimate can be wrong by an order of magnitude. The **$\tau$** measured for the Preprototype sample is 18 msec after cycling, comparable to that calculated above. The Preprototype conductor was not solder-filled, however.

The power deposited per unit volume in the conductor for a given $n\tau$ can then be estimated with:

$p = n\tau/(8\mu_0)(\Delta B)^2\omega^2$ ($W/m^3$),
where $\Delta B$~0.35 T (peak-to-peak), $\omega=2\pi f$, f=2.5 Hz and $n\tau$ ~10msec gives a heat dissipation of **p~38 kW/m$^3$**.

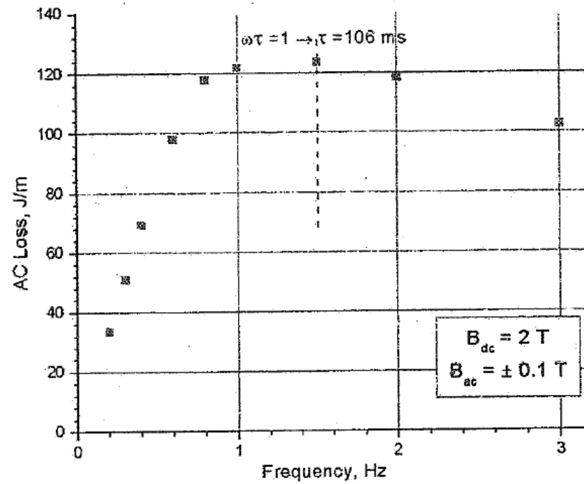


**Figure 23: AC loss data for the CRPP flat cable.**

## 4.2) Thermal Simulation of the EFDA Dipole with Soldered Cable

**Concentrating the pressurized helium in the central conduit reduces the cooling characteristics of the conductor, rendering more difficult the evacuation of heat from the strands. The Cagliari group[11] conducted a thermal finite element model analysis to estimate the temperature drop between the helium and the strands as a result of the thermal impedance of the steel pipe wall and the solder-filled conductor. The thermal conductivities used in the model are given in Figure 24. The low temperature thermal conductivity of the solder was assumed to be 10 W/K/m (see**

Table 3), ~20 times larger than that of the steel at 4 K. The thermal properties of the solder-strand composite was calculated from a simple rule of mixture for the 30/70 volume ratio. The thermal conductivity of the solder-filled cable is obviously dominated by that of Cu. The interface conductance, h, from the 2 mm ID steel pipe inner wall to the flowing, pressurized helium was calculated with Dittus Boelter from the parameters given in Table 7.

The FE model data shown in Figure 25 indicate that the thermal impedance represented by the 0.4 mm steel pipe wall by far dominates the thermal problem. Practically all the temperature drop (4 K) is concentrated there. As can be seen in Figure 26, there is practically no temperature gradient within the soldered conductor block and the solder thermal conductivity therefore is sufficient to assure a good heat exchange. The situation is also not strongly dependent on the helium cooling coefficient. The FE model assumed a heat dissipation of 360 kW/m$^3$ indicates that the thermal impedance of the cooling tube wall would hold the conductor temperature at 9.66K. A different material is needed for the cooling pipe in this case. Also note that the AC-losses estimated in the above section 4.1) is ten times smaller than the one assumed in the FE model. Also the reduced heat load will, of course, strongly reduce the conductor temperature.

[11] P. Testoni and F. Cau, University of Cagliari, Italy.

**Table 7: Parameters used in the calculation of the coefficient for the heat transfer to pressurized helium using the Dittus Boelter relation.**

| Parameter | Unit | Value |
|---|---|---|
| Inner pipe diameter | (mm) | 2 |
| Working pressure | (bar) | 5 |
| Working temperature | (K) | 5 |
| Mass flow | (g/s) | 2 |
| Helium density | (kg/m$^3$) | 129 |
| Helium conductivity | (W/K/m) | 2.2 |
| Helium viscosity | (Pa-s) | $3.5 \cdot 10^{-6}$ |
| Helium specific heat | (J/K/kg) | 4900 |
| Helium speed | (m/s) | 5 |
| Reynolds number | | $3.6 \cdot 10^{5}$ |
| Prandtl number | | 0.8 |
| Nusselt number ($0.023*Re^{0.8}*Pr^{0.4}$) | | 585 |
| Heat transfer coefficient h=Nu*k/D (W/K/m$^2$) | | 6300 |

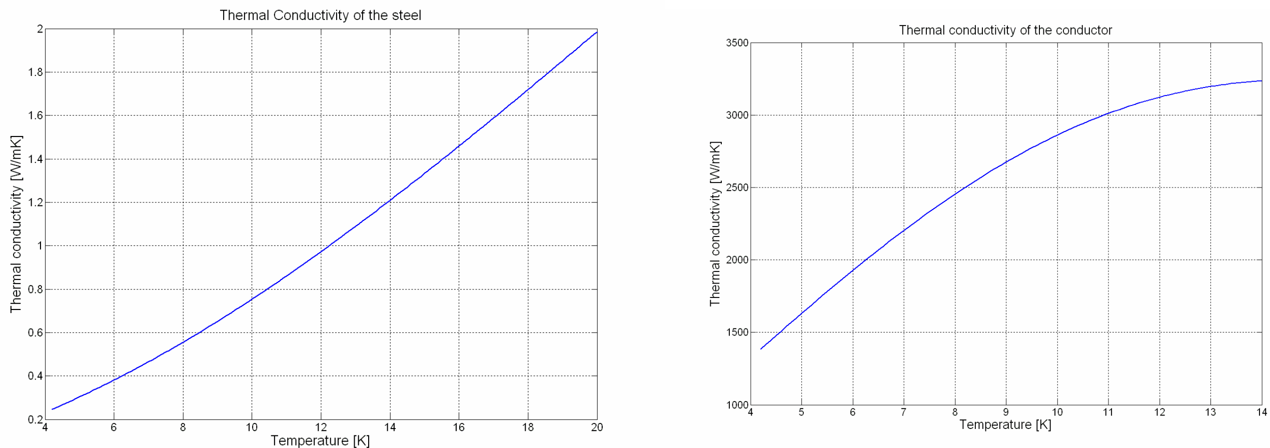


**Figure 24: Thermal conductivity of conduit and cable[12].**

An analytical estimate of the power that can be transferred from the conductor if the cooling tube is removed can be obtained from:

$q=h(\Delta T)d\,\pi / A$ (W/m$^3$),

where $\Delta T \sim 1$ K (temperature drop on interface to pressurized helium) for a **q=360 kW/ m$^3$**, which is 10 times less as computed with the FE model. For this calculation the helium channel diameter is d=2 mm, A=100 mm$^2$ (cross-sectional area of conductor without jacket), and *h=6 kW/m$^2$/K* as calculated in Table 7 (interface conductance). Note that this power is ten times larger than the worst case AC loss calculated in 4.1.

The results of the thermal calculation indicate that the cooling characteristics of the soldered conductor are strongly reduced as compared to those of the conductor with the original design

[12] ITER DRG1 Annex, “Superconducting Material Database”, Art. 5. Thermal, Electrical and Mechanical Properties of Materials at Cryogenic Temperatures. ITER N 11 FDR 42 01-07-05 R 0.1,

(direct cooling through voids). The thermal bottleneck, however, is not the solder, but the stainless steel cooling tube.

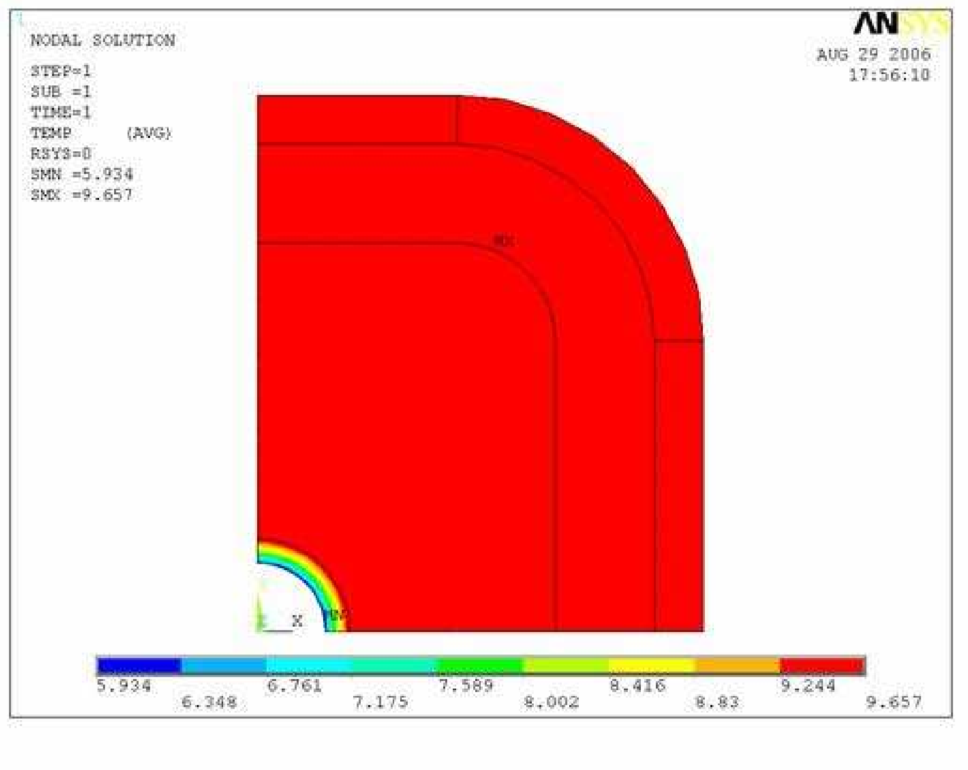


**Figure 25: Results of finite element model of solder filled with heat load Q=360kW/m3 dissipated in the conductor. Only one quadrant of the conductor is shown. The cooling tube is in the middle.**

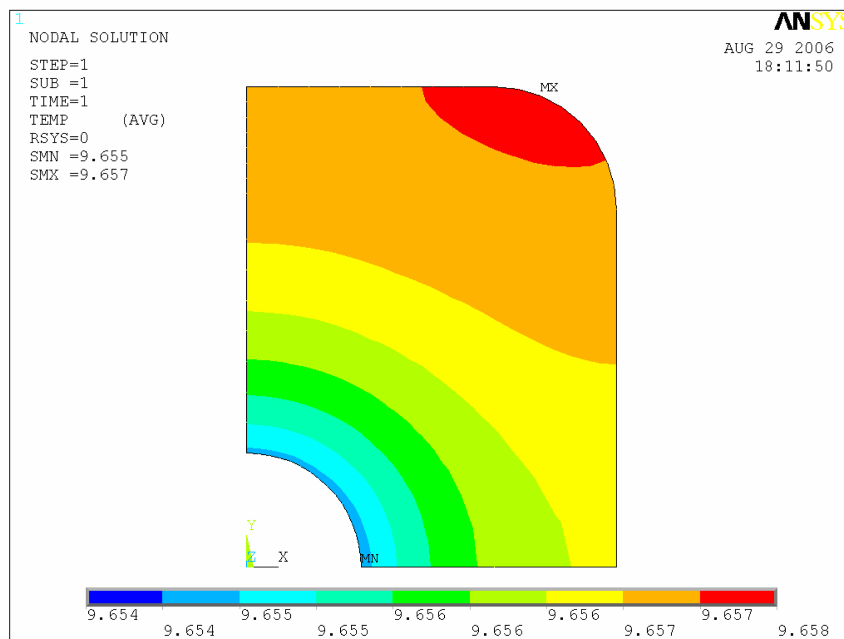


**Figure 26: Temperature distribution in the conductor**

## 4.3) Mechanical Simulation of the EFDA Dipole with Soldered Cable

Solder filling the cable also has consequences for the stresses on the cable within the jacket. Normally the transverse modulus of the multiply twisted fusion magnet cables is measured to be fairly low (a few GPa). In filled conductors, however, the cumulative load from the winding pack will also be felt inside the conductor, depending on the increased modulus of the solder filled cable. The Cagliari group performed a FE model analysis to estimate the peak pressure seen in the conductor as a result of this effect. The winding pack design for this model is the vs 11 design (Figure 22). The material parameters assumed are listed in Table 8. The results of the FE modelling indicate that the peak stress in the solder filled cable can be ~100-200 MPa, depending on whether the filler modulus is low (yielding of the solder, Figure 27) or high (70% Nb3Sn strand and 30% solder = 88 GPa, Figure 28). This pressure is high, even if the strands are well supported by the solder environment. Peak pressures achieved without noticeable degradation in high energy physics high field Nb3Sn magnets were estimated to be 180 MPa[13].

COMPARE THESE VALUES WITH ESTIMATED FILLER MODULUS –

Another, albeit less important, issue is the increased pre-strain in Nb3Sn filaments after cool-down as a result of the additional material in the cable cross-section that is shrinking more than the Nb3Sn. Although the yield strength of the solder is quite low and so this effect small, the solder can also act on the Nb3Sn pre-compression by preventing the cable relaxation during the thermal shrinkage. Additional pre-compression of the Nb3Sn will further reduce the critical current density in the superconductor.

**Table 8: Material properties for mechanical modelling of the EFDA dipole**

| | E (4.2 K) Young modulus at cryo temp | Y (~4.2 K) Yield strength at cryogenic temperature | α (450-4.2 K) integrated thermal expansion | Comment |
|---|---|---|---|---|
| | (GPa) | (MPa) | (%) | |
| 316 LN jacket (Sandvik) | 202 (7 K)[2] | 1100[2] | 0.6[4] | Aged (200h/650C) |
| 316 LN shell (Valinox) | 203 (7 K)[2] | 1232[2] | 0.6[4] (0.46[6]) | Not aged |
| Yoke steel | ~205[1] | 720-920[1] (ultimate) | 0.31[6] | as in LHC dipole (yield at RT: 170 MPa[5]) |
| G10 | 36[3] (20/10 – ITER Specification) | ? | 1.05[4] | Max shear 85 MPa, contraction smaller in direction of fibres |
| Epoxy | 4.3 (300 K) | ? | ? | |
| Strand | 115 GPa[7] (77 K) | 80 MPa (Cu only) | 0.275[8] | usually only the Cu yields |
| Solder | 25 GPa (300 K) | 40 MPa (300 K!) | 0.75 | Sn63Pb37 eutectic |

1 A. Nyilas, FZK, Cern data on LHC Dipole Materials
2 A. Nyilas, FZK, 05/97, "Final Report on Characterization of Jacket Material, Contract NET/96-408
3 ITER- N11 FDR 42 01-07-05 R 0.1 Annex to DRG1, Superconducting Material Database Article 5, Thermal, Electrical and Mechanical Properties of Materials at Cryogenic Temperatures
4 R. Maix, personal data collection from DDD docs
5 G. Peiro, T. Verbeeck et al. "Towards the Production of 50000 Tonnes of Low Carbon Steel sheet for the LHC Superconducting Dipole and Quadrupole Magnets", LHC Report 548, http://documents.cern.ch/archive/electronic/cern/preprint/lhc/lhc-project-report-548.pdf)

[13] A.R. Hafalia et al., "HD1: Design and Fabrication of a 16 T Nb3Sn Dipole Magnet", IEEE Trans. On Appl. Supercond. Vol. 14, No. 2, June 2004; D. Dietderich et al., "Critical Current of SC Rutherford Cable in High Magnetic Field with Transverse Pressure".

6 R. Vuillermet/Cern, “Comparative Study of Different Designs of the MechanicalStructure for the LHC Main Dipoles”, LHC Report 288, http://documents.cern.ch/archive/electronic/cern/LHC/Note/project-note-288.pdf

7 Measurement by strand vendor (OST)

8 Calculated from elemental contraction using “glued beam” model, assuming a reduced modulus of Cu (20) to account for yielding


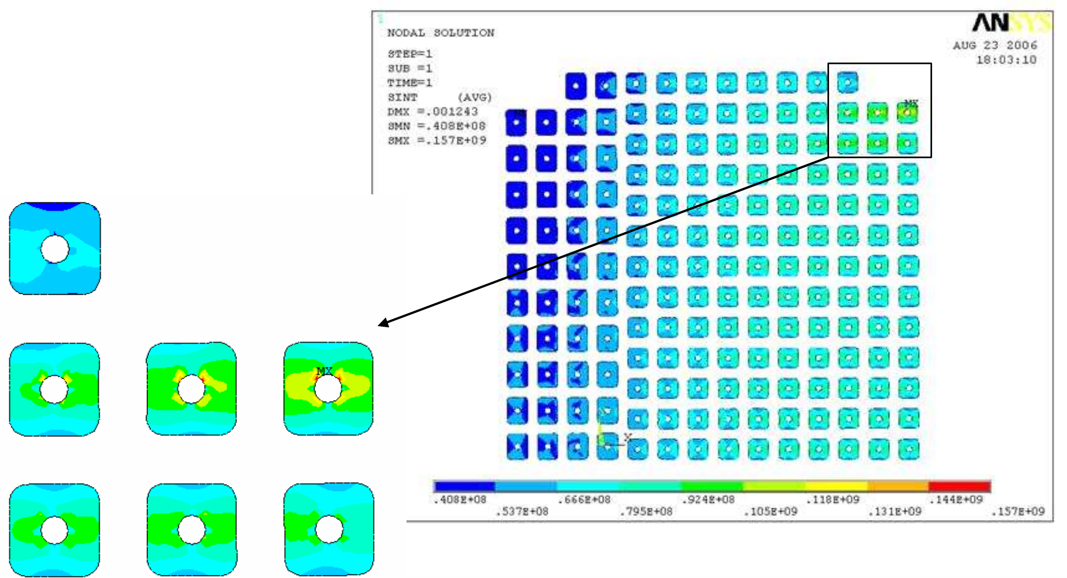


**Figure 27: Pressure in “filler”(=solder-filled cable) in Version 11 of the EFDA dipole for a modulus of 25 GPa.**

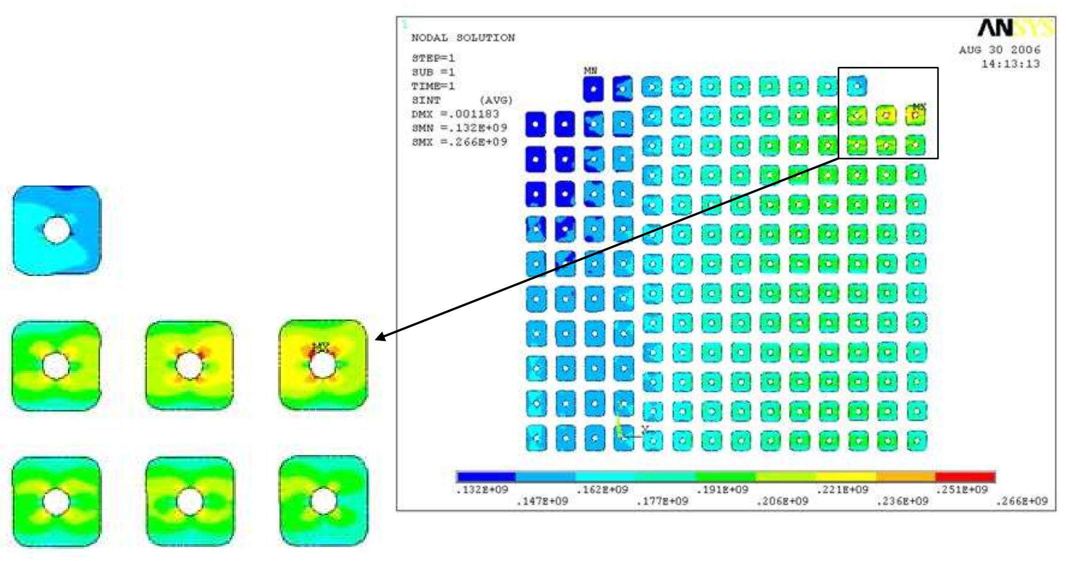


**Figure 28: Pressure in “filler”(=solder-filled cable) in Version 11 of the EFDA dipole for a modulus of 88 GPa.**

# 5) Appendix

## 5.1) Solder companies contacted

Stannol GmBH
Oskarstrasse 3-7
42283 Wuppertal
www.stannol.de
++49 (0)202 585-0

Fonda AG
Riburgerstr. 686
CH-4313 Moehlin
++41-61-855 9999